NONLINEAR RESPONSE SPECTRA FOR PROBABILISTIC SEISMIC DESIGN OF REINFORCED CONCRETE STRUCTURES

Masaya Murakami[I] and Joseph Pênzien[II]

SYNOPSIS

Twenty each of five different types of artificial earthquake accelerograms were generated for computing nonlinear response spectra of five structural models representing reinforced concrete buildings. To serve as a basis for probabilistic design, mean values and standard deviations of ductility factors were determined for each model having a range of prescribed strength values and having a range of natural periods. Adopting a standard design philosophy, required strength levels were investigated for each model. Selected results obtained in the overall investigation are presented and interpreted in terms of prototype behavior.

INTRODUCTION

The general philosophy of seismic resistant design in most countries of the world is that only minor damage is acceptable in buildings subjected to moderate earthquake conditions and that total damage or complete failure should be prevented under severe earthquake conditions. Usually, this design philosophy is applied to performance assessments and to design in a deterministic manner. It should be recognized however that due to the highly variable characteristics of ground motions, even for a given site, as well as the variable properties of structures, large uncertainties exist in predicting structural response. Therefore, nondeterministic methods which formally recognize these uncertainties should be used leading to response predictions in probabilistic terms.

Since it was the intent of this investigation to concentrate on the influence of variability of ground motions on the behavior of reinforced concrete buildings, nondeterministic response analyses were carried out using a stochastic model to represent the expected ground motions. The particular model used is essentially nonstationary filtered white noise as commonly used by many investigators [1,2,3,4]. While this model is admittedly not perfect, it does reflect the main statistical features of real ground motions; therefore, its use in seismic response analyses leads to more realistic predictions than does a single fully prescribed accelerogram.

ARTIFICIAL EARTHQUAKE ACCELEROGRAMS

Five specific types (Types A, B, B_{02}, C, and D) of artificial accelerograms were generated using a modified version of the program (PSEGCN) [1,5], where stationary wave forms having a constant power spectral density function (white noise) of intensity S_0 were modified by multiplying by a prescribed time intensity function, passing the resulting wave forms through both high and low frequency filters, and finally by applying a baseline correction in accordance with the procedure of Berg and Housner [6].

I Associate Professor of Architectural Engineering, Chiba University, Japan
II Professor of Structural Engineering, University of California, Berkeley, U.S.A.

Five time intensity functions were used as shown in Fig. 1. These functions are identical to those used previously by Jennings, et al. [2]. The selected high frequency filter function is plotted in Fig. 2a for ω_o = 15.6 rad/sec and ξ_o = 0.6. These same values of ω_o and ξ_o were used for four of the five classes of accelerograms, namely, Types A, B, C and D. Accelerograms Type B_{02} used the same value for ω_o, i.e. 15.6, but a different value for ξ_o, namely 0.2. The low frequency filter function used is shown in Fig. 2b. The values of T_f used in this function were 7 seconds for Types A, B, B_{02} and 2 seconds for Types C and D following the suggestion of Jennings, et al.[2].

The constant power spectral intensity S_o, used in generating the stationary wave forms, was assigned the value 0.8952 ft^2/sec^3. Table 1 lists the mean values and standard deviations for the peak accelerations in all five classes of accelerograms. The mean values and standard deviations for the infinite number of accelerograms of each class were estimated in accordance with the method of Gumbel [7]. In view of this mean peak acceleration and the time intensity function used, the Type B accelerograms closely represent that class of motions containing the N-S component of acceleration recorded during the 1940 El Centro, California, earthquake [2,3].

STRUCTURAL MODELS

A. ORIGIN-ORIENTED HYSTERETIC MODEL

One of the five structural models used in this investigation was the so-called "Origin-Oriented" hysteretic model proposed by Umemura, et al. [8]. This model is shown in Fig. 3 where it is characterized by p_{sc}, p_{sy}, v_{sc}, and v_{sy} which represent the concrete shear cracking strength, the ultimate shear strength, the relative displacement produced by p_{sc}, and the relative displacement produced by p_{sy}, respectively. Two other parameters are used in generating response spectra, namely, period $T_1 = \sqrt{m/k_1}$ and ratio $(p_{sc}/m\ddot{v}_{go})$ where m is the mass of the single degree of freedom system and $\ddot{v}_{go}$ is the mean peak ground acceleration. Through the use of this ratio, the absolute values of mean peak acceleration shown in Table 1 need not be specified separately.

B. TRILINEAR STIFFNESS DEGRADING HYSTERETIC MODEL

Four of the five structural models used in this investigation were the so-called "Trilinear Stiffness Degrading" hysteretic model [8]. This model is shown in Fig. 4 where it is characterized by p_{Bc}, p_{By}, v_{Bc}, and v_{By} which represent the load at which the concrete cracks due to flexure, the load at which the main reinforcing steel starts yielding due to flexure, the relative displacement produced by p_{Bc}, and the relative displacement produced by p_{By}, respectively. As in the case of the origin-oriented model, two other parameters are used in generating response spectra, namely, period $T_1 = \sqrt{m/k_1}$ and ratio $(p_{By}/m\ddot{v}_{go})$.

One characteristic feature of the trilinear stiffness degrading model worth noting is that when subjected to full-reversal cyclic displacements at a constant amplitude the bilinear hysteretic loops are perfectly stable. Using period $T_2 \equiv 2\pi\sqrt{m/k_y}$ one can calculate the equivalent damping ratio ξ_e for a linear viscously-damped single degree system which represents the same energy absorption per cycle of oscillation. This damping ratio is shown in

Fig. 5 for each of four different bylinear models together with the parameters of each model.

DUCTILITY RESPONSE SPECTRA

Mean maximum ductility factors $\bar{\mu}$ and their corresponding coefficients of variation were generated for the origin-oriented shear model and the four trilinear stiffness degrading flexure models using the 20 response time histories for each class of earthquake ground motions. Two examples of the results obtained are shown in Figs. 6 and 7 for the origin-oriented models and for one of the four trilinear models, respectively, when subjected to Type A excitations.

For each type of earthquake excitation, the maximum ductility factors generally increase with decreasing period and the spread of these ductility factors over the full strength range increases with decreasing period. Also these ductility factors for a fixed period increase with decreasing structural strength. The trends of the coefficients of variation for the maximum ductility factors with period are similar to the trends just described for mean maximum ductility factor, particularly regarding strength level and strength variation. It is most significant to note that the coefficients of variation are low when the response is essentially elastic ($\mu < 1$) but they can become very large with increasing inelastic deformations.

USE OF DUCTILITY RESPONSE SPECTRA FOR PROBABILISTIC SEISMIC DESIGN

A. *SELECTION OF REQUIRED DUCTILITY LEVELS*

Previous investigations have shown that the probability distribution function for extreme value of structural response for a single class of earthquakes follows closely the Gumbel Type 1 distribution [1,3]

$$P(\mu) = \exp \{- \exp [- \alpha (\mu - u)]\} \qquad (1)$$

where μ is the maximum response measured in terms of ductility factor, and α and u are parameters which depend on the average and standard deviation of μ. If only 20 sample values of μ are available as in this investigation, α and u can be obtained using the relations [7]

$$\alpha = 1.063/\sigma_{\mu} \quad \text{and} \quad u = \bar{\mu} - 0.493\, \sigma_{\mu} \qquad (2)$$

Suppose for example, it was decided that a 15 percent probability of exceedance was acceptable, i.e. $P(\mu) = 0.85$. Using Eq. (1) and the data provided in Figs. 6-7, one can easily establish that ductility factor μ_{85} associated with $P(\mu) = 0.85$. This has been done for two trilinear stiffness degrading models subjected to Type A ground motions giving the results shown in Fig. 8.

B. SELECTION OF REQUIRED STRENGTH LEVELS

To establish the required strength levels of the various structural models for each class of earthquake motions, one must first prescribe basic criteria consistent with the basic design philosophy. It will be assumed

that moderate and severe earthquake conditions are represented by 0.30g and 0.45g, respectively, for the corresponding peak ground accelerations. Further, the two ductility factors, consistent with light and heavy (but controlled) damage, are chosen as 2 and 10 for the origin-oriented shear model and 2 and 4 for the trilinear stiffness degrading model. The values of mean peak accelerations and ductility factors selected above follow the suggestions of Umemura, et al. [8].

Using data such as shown in Fig. 8 for each structural model and for each type of earthquake motion, i.e. using curves of μ_{85} vs. T_1, one can easily obtain the required strength ratios ($\beta \equiv p_y/m\ \ddot{v}_{go}$) for discrete values of T_1. Linear interpolation between the curves (μ_{85} vs. T_1) for a fixed value of T_1 can be used for this evaluation. The resulting required strength ratios can then be plotted as functions of period T_1 as shown in Fig. 9. When judging which of the two prescribed ductility factors control a particular design, one should be careful not to base the decision on a direct comparison of the required strength ratios as shown in Fig. 9, but to select the larger of the two strength ratios required to satisfy the prescribed maximum ductility factors under moderate and severe earthquake conditions. The required strength ratios for the trilinear models are shown only for $\mu_{85} = 4$ since the heavy damage criterion always controls the design.

Two characteristic features shown in Fig. 9 are that the four curves representing earthquake Types A, B, C, and D are quite close together in each case showing that the influence of duration of ground motions is not large, and that the required strength ratios for relatively larger periods vary in a linear manner with negative slopes along the log scale for T_1, i.e. converting to a linear scale, the strength ratios would vary in inverse proportion to the square root of T_1.

One significant feature shown in Fig. 1 where the required strength ratios are plotted as functions of periods T_2, is that the ratios vary considerably with period T_2 and the equivalent damping ratio ξ_e (see Fig. 5); therefore, these two parameters are important to the seismic response of reinforced concrete structures of the flexural failure type.

When using the results in Figs. 9 and 10, one should remember that they are based on the ground motion parameters $\omega_o = 15.6$ rad/sec ($T_o = 0.4$ sec) and $\xi_o = 0.6$ which represent firm ground conditions. If one should have quite different ground conditions, these parameters should be adjusted appropriately. These adjustments shift the level of the predominant frequencies in the ground motions and also change the mean intensity level $\ddot{v}_{go}$. With considerable experience and using engineering judgment, certain modifications to the data in Figs. 9 and 10 can be made to reflect these new conditions.

CONCLUDING STATEMENT

The mean maximum ductility factors and their corresponding coefficients of variation presented herein provide the necessary data for carrying out probabilistic seismic resistant designs consistent with basic design criteria and the statistical nature of earthquake ground motions.

ACKNOWLEDGMENT

The authors express their sincere thanks and appreciation to the National Science Foundation for its financial support of this investigation.

BIBLIOGRAPHY

[1] Ruiz, P., and Penzien, J., "Probabilistic Study of the Behavior of Structures during Earthquakes," Earthquake Engineering Research Center, No. EERC 69-3, University of California, Berkeley, California, March, 1969.

[2] Jennings, P. C., Housner, G. W., and Tsai, N. C., "Simulated Earthquake Motions," Earthquake Engineering Research Laboratory, California Institute of Technology, Pasadena, California, April, 1968.

[3] Penzien, J., and Liu, S-C., "Nondeterministic Analysis of Nonlinear Structures Subjected to Earthquake Exitations," Proceedings of the 4th World Conference on Earthquake Engineering, Santiago, Chile, January, 1969.

[4] Amin, M., and Ang, A. H. S., "A Nonstationary Stochastic Model for Strong-Motion Earthquake," Structure Research Series 306, University of Illinois, Urbana, Illinois, April, 1966.

[5] Murakami, M., and Penzien, J., "Nonlinear Response Spectra for Probabilistic Seismic Design and Damage Assessment of Reinforced Concrete Structures," Earthquake Engineering Research Center, No. EERC 75-38, University of California, Berkeley, 1976.

[6] Berg, G. V., and Housner, G. W., "Integrated Velocity and Displacement of Strong Earthquake Ground Motion," Bulletin of the Seismological Society of America, Vol. 51, No. 2, April, 1961.

[7] Gumbel, E. J., and Carlson, P. G., "Extreme Values in Aeronautics," Journal of the Aeronautical Sciences, 21, No. 6, June, 1954.

[8] Umemura, H., et. al., "Earthquake Resistant Design of Reinforced Concrete Buildings, Accounting for the Dynamic Effects of Earthquake," Giho-Do, Tokyo, Japan, 1973 (in Japanese).

TABLE 1

MEAN VALUES AND STANDARD DEVIATIONS OF PEAK GROUND ACCELERATIONS

Type of Earthquake	Statistical Quantity	Number of Earthquakes		
		20	40	Infinity
A	Mean	0.327	0.331	0.332
	Std. Deviation	0.023	0.036	0.040
B	Mean	0.300	0.308	0.309
	Std. Deviation	0.032	0.037	0.041
C	Mean	0.240	0.243	0.244
	Std. Deviation	0.022	0.035	0.039
D	Mean	0.191	0.188	0.189
	Std. Deviation	0.041	0.039	0.044
B_{02}	Mean	0.346	0.336	0.337
	Std. Deviation	0.048	0.049	0.055

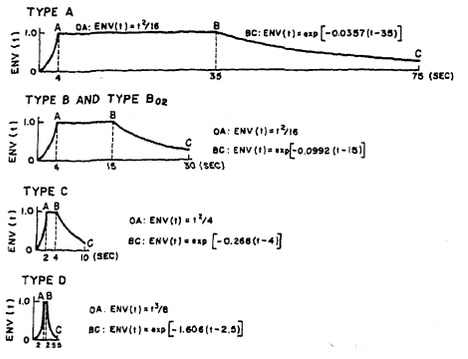

Fig. 1 Time Intensity Functions

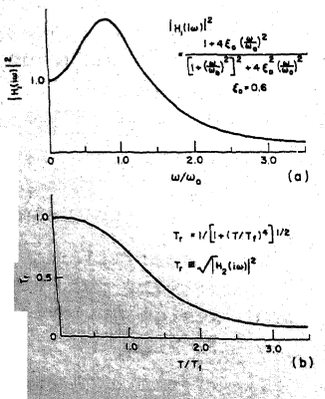

Fig. 2 Filter Transfer Functions

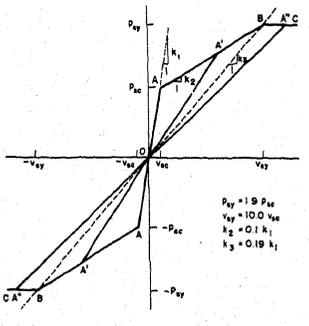

Fig. 3 Origin-Oriented Hysteretic Model

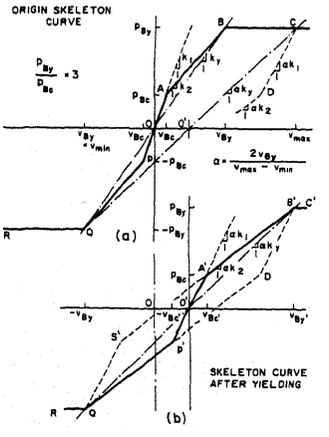

Fig. 4 Trilinear Hysteretic Model

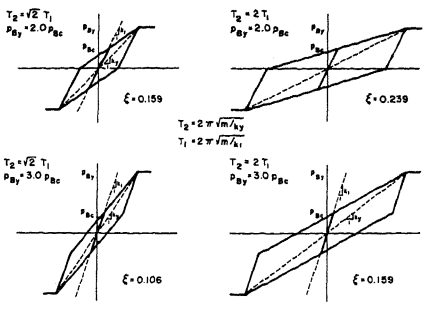

Fig. 5 Stable Bilinear Hysteretic Loop for Trilinear Stiffness Degrading Model

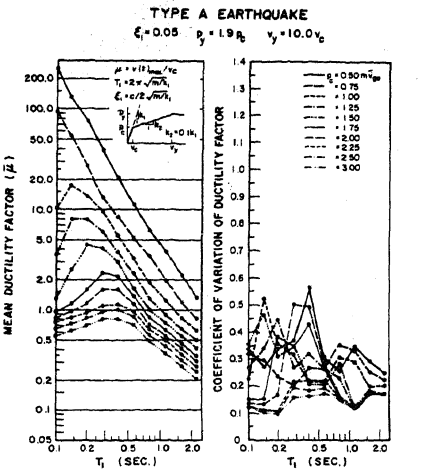

Fig. 6 Mean Ductility Factors and Corresponding Coefficients of Variation for Origin-Oriented Model

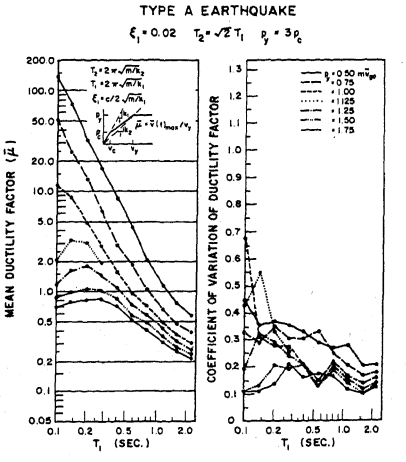

Fig. 7 Mean Ductility Factors and Corresponding Coefficients of Variation for Trilinear Stiffness Degrading Model

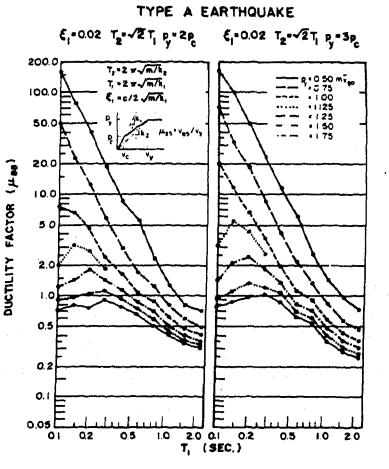

Fig. 8 Response Ductility Factors for 85% Level on Probability Distribution Functions

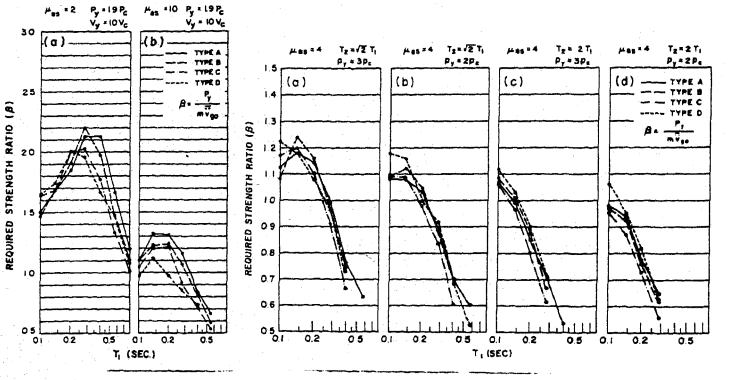

Fig. 9 Required Strength Ratios for Origin-Oriented Model and Trilinear Stiffness Degrading Models at the 85 % Probability Distribution Level

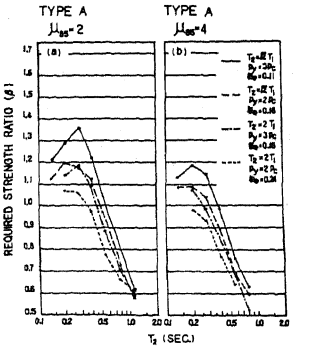

Fig. 10 Required Strength Ratios vs. T_2 for Trilinear Stiffness Degrading Models at the 85 % Probability Distribution Level